# Multiband Spectrum Sensing via Edge Detection Using a Wavelet Approach

Ricardo Tadashi Kobayashi, Lucas Claudino, Aislan Gabriel Hernandes and Taufik Abrão

***Abstract*— In cognitive radio (CR), the sensed aggregate bandwidth could be as large as several GHz. This is especially challenging if the bandwidths and central frequencies of the sensed signals are unknown and need to be detected. This work discusses a new method for multi-band spectrum-sensing based in edge detection. The proposed method uses a Welch power-spectrum-density (PSd) estimate and a multi-scale Wavelet approach to reveal the spectrum transition (edges), which is deployed to characterize the spectrum occupancy in CR scenarios where the operating frequency limits of the primary users are unknown. The focus in this work is to improve the performance of the multiband spectrum sensor by refining the edge location and error correcting misleading detections. In order to do so, a comprehensive analytical description and numerical analysis have been carried out by focusing on orthogonal-frequency-division-multiplexing (OFDM) signals. Also, numerical results corroborate and give support to the effectiveness of the proposed multiband spectrum sensing method.**

**Keywords. Cognitive radio, multiband spectrum sensing, Gaussian filtering, Welch PSD estimation.**

## I. Introduction

Over the past decades, spectrum scarcity has become one of, if not the, the greatest challenges on telecommunication systems, given the massive number of users and their stringent requirements. A possible solution for this spectrum scarcity can be achieved through its efficient usage [1]. Some promising solutions, to name a few, include multiple antenna systems (MIMO, Multiple-Input and Multiple-Output systems), mmWaves and CRs.

Through the use of a large number of antennas, MIMO systems can achieve expressive spectral and energy efficiency gains, but at a higher cost and a more complex implementation [2]. Sharing similar problems, systems operating in mmWaves convey information in frequencies higher than 30GHz. In fact, MIMO systems and mmWaves can be combined in order to circumvent their drawbacks [3]. On the other hand, CR is a much less explored topic with many study possibilities. A CR can be generically defined as a system capable of adapting itself dynamically according to the environment, aiming to make the best use of the scarce resources available, specially spectrum and power/energy. To do so, a CR must make a real time interaction in order to operate intelligently to maximize its performance [4], [5], requiring capabilities like learning, adaptability and management.

As expected, CRs must sense the spectrum, seeking idle bands in order to make an opportunistic usage of this resource. Through spectrum sensing, unlicensed users, or secondary users (SU), are allocated to unused bands, without interfering users who own that spectrum range, i.e., primary users (PU). Despite being a controversial subject, it is a promising idea since a substantial portion of the spectrum remains unused most of the time [6].

The authors are with the Communications Group, Department of Electrical Engineering, Londrina State University, Paraná, Brazil. Emails: {ricardokobayashi.9107,lsclaudino,aislangabrielhernandes}@gmail.com; @gmail.com; @gmail.com; taufik@uel.br.

As spectrum sensing plays an important role in CRs, many sensing techniques have already been proposed. For single-band sensing, techniques such as energy-detector, matched-filter and cyclostationary detector are available [7]. However, multiple single-band sensors must be deployed in order to sense a wide bandwidth or to determine spectrum usage with accuracy. Multiband spectrum sensing techniques can circumvent these drawbacks, enabling non-contiguous spectrum allocation. Multiband spectrum sensors can deploy multiple antennas [8], [9], compressive sensing [9] and edge detection via wavelets [10], [11].

In this work, a multiband spectrum sensing based on the wavelet approach is proposed and characterized. Basically, the proposed method consists in a filter bank, resembling the components of a wavelet, a network capable of detecting spectrum edges, an edge classifier and a spectrum mask estimator. In comparison to other works, this work introduces a simple, yet effective, topology to detect and classify spectral transition from the filter bank. As it will be demonstrated by simulation, the proposed method has demonstrated efficiency, even when operating under low SNR, to determine the PU's spectrum usage. In special, this paper exemplifies the operation and effectiveness of the proposed method when OFDM signals are deployed.

The remaining work is organized as follows: section II presents the system model; section III describes the proposed method; section IV exemplifies the operation of the spectrum sensing techniques; section V offer conclusions and final remarks.

**Notation:** $\delta(t)$ and $u(t)$ denotes the impulse and step function, respectively. The derivative of $f(t)$ is denoted by $f'(t)$; $z^{-1}$ represents unitary sample delay; $*$ is the convolution operator and estimated values are denoted by the $\widehat{(\cdot)}$.

## II. System Model

For this work, consider that an SU receiver is designed to sense the presence of $N_u$ primary-users with non-overlapping spectrum. The spectrum usage will be estimated based on the received signal:

$$x(t) = \sum_{i=1}^{N_u} h_i s_i(t) + n(t), \tag{1}$$

where $h_i = \{0, 1\}$ define whether or not the $i$-th user is active; $s_i(t)$ is the $i$-th signal which occupies a respective sub-band

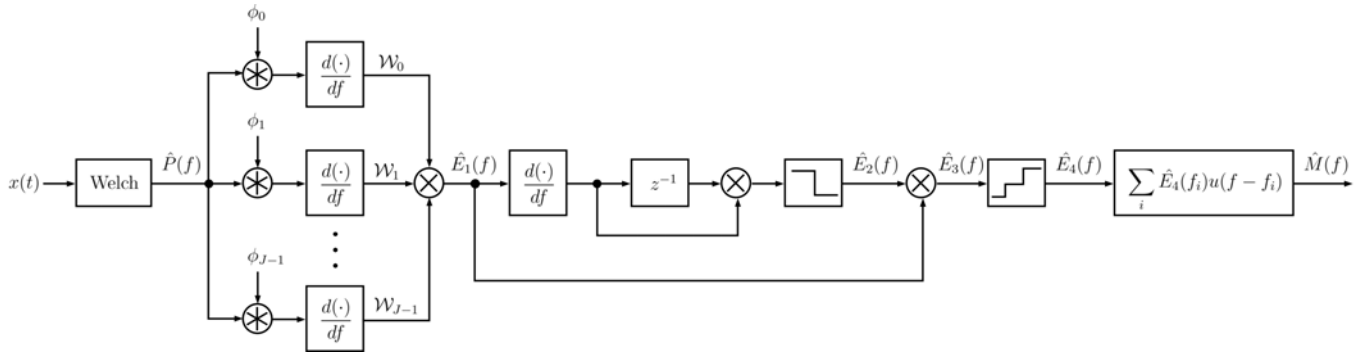


Fig. 1. Diagram block for the proposed spectrum sensing method.

$BW_i$; and $n(t)$ is the additive noise. One of the SU tasks is to determine the exact bandwidth and the carrier position of each PU. Based on this spectrum estimate, the CR system is able to allocate free sub-bands to other secondary users, aiming to maximize the overall spectral efficiency.

## III. Proposed Multiband Spectrum Sensing Method

The proposed multi-band spectrum sensing method presented in this work is summarized in the block diagram of Fig. 1. Basically, this technique estimates the PSD of the sensed band, finds the edges of the signal spectrum through multi filtering by a Gaussian filter bank and finally it generates a spectrum mask of the occupied sub-bands. A detailed description of this method is explored in the sequel and includes a) PSD estimation block, b)-c) edge detection I and II, d) edge classifier block, e) error correction block, and f) spectral mask generator,

### A. PSD Estimation

In order to obtain the PSD estimate of the received signal, this work will deploy the Welch method [12], [13]. In this method, the periodogram of the received signal, sampled at a rate $f_s = 1/T_s$, is divided into $K$ segments of length $L$, considering that adjacent segments present an overlap of $O$ samples, i.e.,

$$x_j[n] = x[n + (j-1)O], \tag{2}$$

with $n = 0, 1, \cdots L-1$ and $j = 0, 2, \cdots K-1$. After all segments have been determined, the periodogram is calculated by

$$\mathcal{I}_x(f_k) = \frac{1}{N^2 U}\left|\sum_{n=0}^{N-1} x(nT_s)w[n]\exp\left(-j2\pi n\frac{k}{N}\right)\right|^2 \tag{3}$$

where $w[n]$ is the windowing function, the scalar $U$ is defined as

$$U = \frac{1}{N}\sum_{n=0}^{N-1} w^2[n], \tag{4}$$

and the frequencies of the PSD

$$f_k = f_s\frac{k}{N}, \qquad k = 0, 1, \cdots N/2. \tag{5}$$

From the $K$ different sample segments, the Welch PSD estimate can be expressed as

$$\hat{P}(f_k) = \frac{1}{K}\sum_{j=1}^{K}\mathcal{I}_{x_j}(f_k), \tag{6}$$

i.e., the average value of each peridogram segment of eq. (3). As the Welch PSD estimate is evaluated over averages, it becomes smoother than the periodogram. Hence, the Welch's estimate is a good alternative for edge detection in wideband spectrum sensing, since a smoother PSD may avoid false edges due to abrupt variations.

### B. Edge detection I

After the PSD estimate is evaluated, it passes through $J$ parallel branches. Each branch filters out and differentiates the PSD estimate, generating the signal

$$\mathcal{W}_i'(f) = \frac{d}{df}\left[\phi_i(f) * \hat{P}(f)\right]. \tag{7}$$

It is necessary to that filtering is done in the frequency domain convoluting the signal PSD with the filter impulsive response. It is also noteworthy mentioning that positive peaks in $\mathcal{W}_i'(f)$ indicate rising edges, while negative peaks indicate falling edges. In order to reduce spurious edge detection, all the branches are multiplied, i.e.,

$$\hat{E}_1(f) = \prod_{i=0}^{J-1}\sqrt{2\pi\sigma_i^2}\mathcal{W}_i'(f). \tag{8}$$

Thus, the main peaks that characterize the edges remain only when they are present in all branches [10], while other local extremes that do not occur in all branches are vanished after the multiplication. A very important detail is that, $J$ must be an odd number, otherwise the negative peaks will be lost, and so the falling edge characterization. Also, as $J$ increases, spurious edge detection decreases due to the product procedure in (8).

Particularly, this work deploys a Gaussian blur filter in order to generate a smoother PSD in adjacent points to spectral edges. different scales $\sigma_i$, which are characterized by the following frequency response

$$\phi_i(f) = \frac{1}{\sqrt{2\pi\sigma_i^2}}\exp\left(-\frac{f^2}{2\sigma_i^2}\right), \ i = 0, 1, \ldots, J-1. \tag{9}$$

Notice that, $\sigma_i$ should not be much larger than the bandwidth of a PU, for it would make difficult the edge characterization. On the other hand, large scales present a poorer filtering, compromising the noise supression [11]. In this sense, this work fixed the scales to

$$\sigma_i = 100 \cdot \frac{f_s}{M} \cdot 2^{-i}, \tag{10}$$

which bounds the scales to the sampling frequency and the number of points of the PSD ($M$).

### C. Edge Detection II

In order to find the exact location of the rising/falling edge in the sensed spectrum, the roots of the derivative of $\hat{E}_1(f)$ are found, in other words,

$$\hat{E}_2(f) = \begin{cases} \delta(f - f_i), & \hat{E}_1'(f_i)\hat{E}_1'(f_i - fs/M) < 0 \\ 0, & \text{otherwise} \end{cases}. \tag{11}$$

Notice that, the above method for finding the edge location is based on the concept of bisection method. In this case, a point of $E_1'$ is multiplied by its neighbor; if the result turns out to be negative, there is a sign transition and a root between these points is present; otherwise, there is no root between the points. Also, at this point, the edges exact location are characterized by unitary impulses.

Even after locating the edges, it is still desirable to preserve the peak intensity of each detected edge, since it must be classified as a falling, rising or a misdetected edge. Therefore, a suitable function is

$$\hat{E}_3(f) = \hat{E}_1(f)\hat{E}_2(f) = \hat{E}_1(f_i)\sum_i \delta(f - f_i), \tag{12}$$

where $f_i$ are the frequencies in which the edges occur.

### D. Edge Classifier

Since the signal is immersed in noise, spurious edge detection may occur and must be rejected as often as possible. In this sense, all the estimated edges should pass through a hard decision with a suitable threshold $\lambda$. Besides, for convenience, the edges will be represented as impulses:

$$\hat{E}_4(f_i) = \begin{cases} \delta(f - f_i), & \hat{E}_3(f_i) > \lambda \\ -\delta(f - f_i), & \hat{E}_3(f_i) < -\lambda \\ 0, & \text{otherwise} \end{cases}, \tag{13}$$

which can be helpful for generating the spectral mask.

### E. Minor Error Corrections

Even after the hard decision stage, misdetected edges are still possible. Nevertheless, they can be reduced by using the fact that two consecutive edges may not present the same sign. Therefore, if a burst of rising edges is detect, the edges from the left side should be eliminated; while if a burst of falling edges occurs, the edges from the right should be eliminated.

Also, if the whole spectrum of the primary users is contained in the range of the spectral sensing, there should be only an even number of edges occurrences. Hence, it is possible to correct the edge misdetection, improving the detector's performance.

### F. Spectral Mask

At last, a two level spectrum mask is generated, where the high states represent occupied sub-bands, while the low state represents idle ones. Since we modeled the edges as impulses, the spectrum mask can be obtained, mathematically, by integrating $\hat{E}_4$:

$$\hat{M}(f) = \int_0^\infty \hat{E}_4(f_i)df = \sum_i \hat{E}_4(f_i)u(f - f_i) \tag{14}$$

## IV. Numerical Results

In this section, numerical results are presented in order to offer a better insight of the operation of the proposed method, beside highlighting the performance of the spectrum sensing technique. For this, the spectrum sensing is performed over OFDM signals with 1024 subcarriers, maximum spectrum overlap[1], 4-QAM (quadrature amplitude modulation) symbols, a bandwidth of 40MHz and a SNR of $-18$dB[2], considering the operating parameter listed in Table I.

| Parameter | Value |
|---|---|
| Sample rate ($f_s$) | $f_s = 1$GHz |
| # segments for PSD estimation ($K$) | $K = 7$ |
| Segment length ($L$) | $L = 2048$ |
| Overlapping samples ($O$) | 1024 |
| $J$ | 3 |
| Threshold ($\lambda$) | $2 \cdot 10^{-9}$ |

TABLE I

Multiband spectrum sensing parameters

First, it will be considered $N_u = 1$, i.e., only one user transmitting in the sensed spectrum range, aiming to demonstrate the whole operation of the technique. The initial stage of the sensing process is the PSD estimation, presented in Fig. 2. As the observation time over the noisy signal is limited, the PSD estimate of the noise cannot be flat, making the spectrum sensing problem more challenging since the noise deteriorates the spectrum content of the ODFM signal.

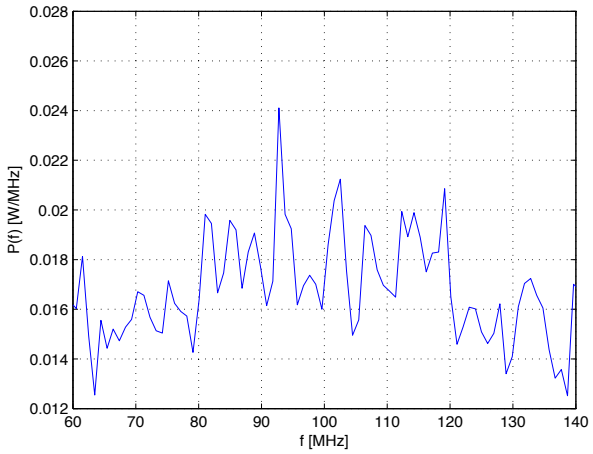


Fig. 2. Noisy PSD estimate.

[1] 50% of spectral overlap between adjacent subcarriers

[2] $SNR_i = \mathbb{E}\left[|s_i(t)|^2\right]/\mathbb{E}\left[|n(t)|^2\right]$

After the PSD estimation, the signal passes through a bank of Gaussian filters, resembling a wavelet transform. This bank filters generates smoother representations of the OFDM spectrum, mitigating the noise, as depicted in Fig. 3. These signals are differentiated and multiplied as stated in (8), producing the waveform presented in Fig. 4. An initial idea of the edges can be extracted from this figure, as its peaks coincide with the edges of the OFDM spectrum. Also, minor peaks which are interpreted as spurious edges were suppressed by the product rule.

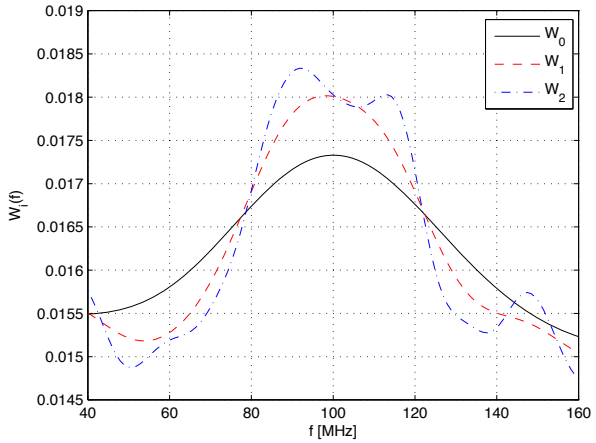


Fig. 3. Filtered PSDs $\mathcal{W}_i$.

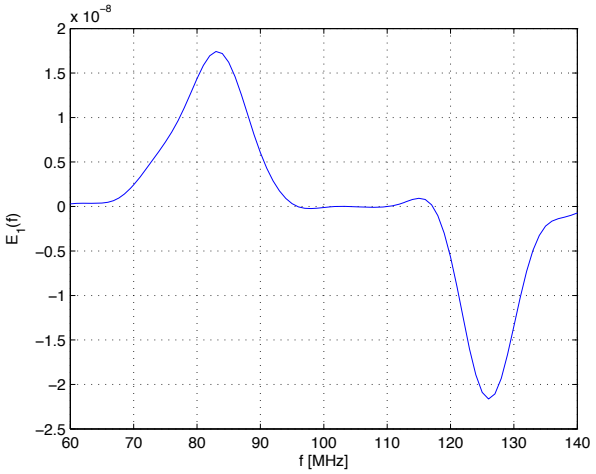


Fig. 4. Signal $\hat{E}_1(f)$, where local extremes are edges.

In order to find the edges of the OFDM spectrum, the peaks of Fig. 4 are evaluated. It can be proceeded by differentiating the signal in Fig. 4 one more time and finding its roots, as presented in Fig. 5 as unit impulses.

The weights of the peaks are then incorporated by multiplying the signals in Fig. 4 and 6, i.e., by multiplying the signals $E_1(f)$ and $E_2(f)$. This waveform (Fig. 7) passes, then, through a hard decision, selecting only the most probable edges, as depicted in Fig. 8. Despite not being explained, a deeper analysis would show that the recommendable threshold for OFDM signals lies around $A^J$, where $A$ is the peak of the OFDM PSD, which may be a drawback for the method as this value is generally unknown.

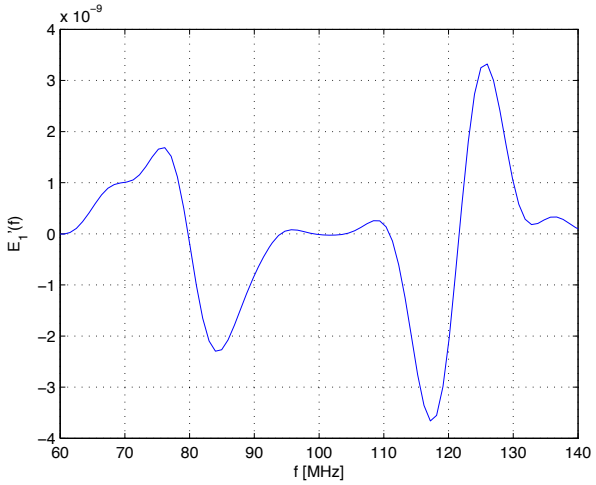


Fig. 5. Derivative of $\hat{E}_1(f)$.

Finally, with the detected edges, the mask of the spectrum used by the PU is generated, as showed in Fig. 9. As observed throughout the sensing procedure, it was possible to make a robust edge detection, even considering low SNRs of order of $-20$dB. However, it is noteworthy that, by making the number of subcarriers high (1024), the PSD estimate of the OFDM signal becomes more uniform, facilitating the detection, as the signal and the noise PSD variations are not heavily combined such that false edges occur.

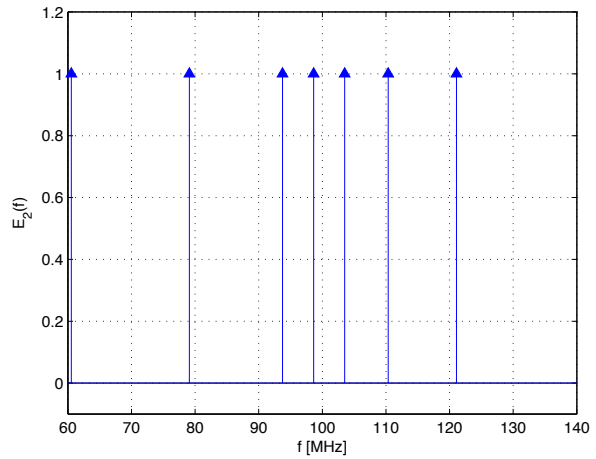


Fig. 6. $\hat{E}_2(f)$, roots of $\hat{E}_1'(f)$, or points where spectrum edges occur.

For the second scenario, it is considered $N_u = 4$ PUs, each one operating with the same signal structure and bandwidth, as in the previous scenario. In this case, the effectiveness of this method in multiband sensing is corroborated in depicted Fig. 10, where the received normalized PSD, the noiseless PSD and the spectral mask of the signal are presented. Even operating under low SNR, it was possible to locate the spectrum usage of each PU with a reasonable accuracy.

## V. Conclusions

Throughout this contribution, it was proposed a multiband spectrum sensing technique based on edge detection of PSD estimates combined with a filter bank topology. In our study,

a detailed description and study of the proposed method was made considering OFDM signals, highlighting each step, their features and some drawbacks. As it was observed, the method has demonstrated robustness under low SNR with OFDM signals, specially when operating under a large number of sub-carriers. Thus, by presenting good performance and accuracy under low SNR and for a wide range of the spectrum, specially with a widespread OFDM waveforms, the proposed method showed to be a robust an attractive choice for multiband spectrum sensing in CRs.

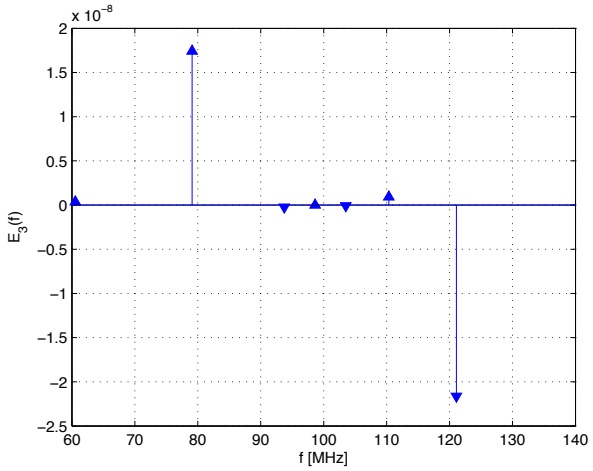


Fig. 7. Signal $\hat{E}_3(f) = \hat{E}_1(f) \cdot \hat{E}_2(f)$.

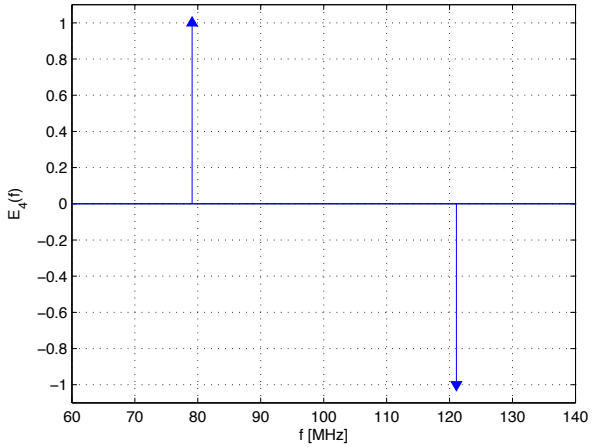


Fig. 8. Signal $\hat{E}_4(f)$, generated after the hard decision, as described in eq. (13).

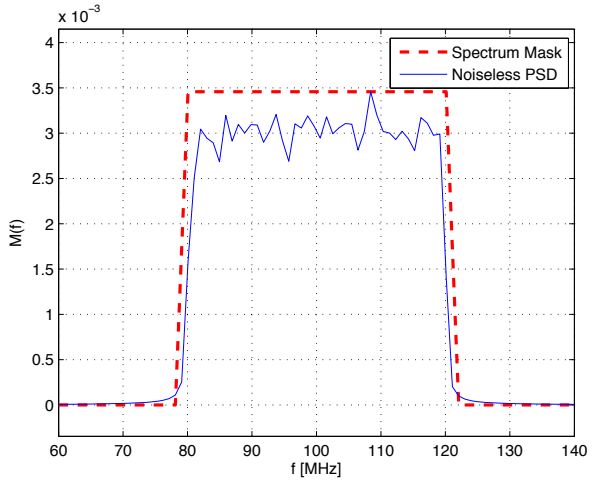


Fig. 9. Final estimated spectrum mask for an OFDM signal.

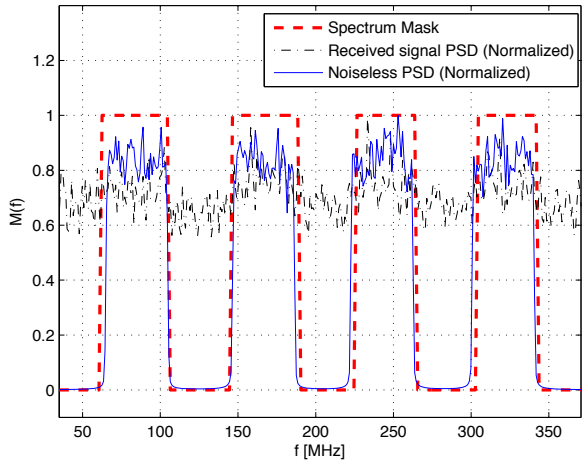


Fig. 10. Estimated spectrum mask for a multiband OFDM signals representing $N_u = 4$ PUs.

## REFERENCES


[1] G. Staple and K. Werbach, "The End of Spectrum Scarcity," *IEEE Spectrum*, vol. 41, no. 3, pp. 48–52, 2004.

[2] F. Rusek, D. Persson, B. K. Lau, E. G. Larsson, T. L. Marzetta, O. Edfors, and F. Tufvesson, "Scaling up MIMO," *IEEE Signal Processing Magazine*, vol. 30, no. 1, pp. 40–60, 2012.

[3] W. Roh, J.-Y. Seol, J. Park, B. Lee, J. Lee, Y. Kim, J. Cho, K. Cheun, and F. Aryanfar, "Millimeter-wave beamforming as an enabling technology for 5g cellular communications: theoretical feasibility and prototype results," *Communications Magazine, IEEE*, vol. 52, no. 2, pp. 106–113, February 2014.

[4] I. F. Akyildiz, W.-Y. Lee, M. C. Vuran, and S. Mohanty, "A survey on spectrum management in cognitive radio networks," *Communications Magazine, IEEE*, vol. 46, no. 4, pp. 40–48, 2008.

[5] M. Masonta, M. Mzyece, and N. Ntlatlapa, "Spectrum Decision in Cognitive Radio Networks: A Survey," *Communications Surveys Tutorials, IEEE*, vol. 15, no. 3, pp. 1088–1107, Third 2013.

[6] S. Haykin, "Cognitive radio: brain-empowered wireless communications," *IEEE Journal on Selected Areas in Communications*, vol. 23, no. 2, pp. 201–220, Feb 2005.

[7] M. Ibnkahla, *Cooperative cognitive radio networks : the complete spectrum cycle*. CRC Press, 2014.

[8] H. Qing, Y. Liu, G. Xie, and J. Gao, "Wideband spectrum sensing for cognitive radios: A multistage wiener filter perspective," *Signal Processing Letters, IEEE*, vol. 22, no. 3, pp. 332–335, March 2015.

[9] H. Sun, A. Nallanathan, C. X. Wang, and Y. Chen, "Wideband spectrum sensing for cognitive radio networks: a survey," *IEEE Wireless Communications*, vol. 20, no. 2, pp. 74–81, April 2013.

[10] Y. Miar and C. D'Amours, "Novel spectrum edge detection techniques in wideband spectrum sensing of cognitive radio," *2011 IEEE 22nd International Symposium on Personal, Indoor and Mobile Radio Communications*, pp. 315–319, 2011.

[11] L. Zhang and P. Bao, "Edge detection by scale multiplication in wavelet domain," *Pattern Recognition Letters*, vol. 23, pp. 1771–1784, 2002.

[12] P. D. Welch, "The use of fast fourier transform for the estimation of power spectra: A method based on time averaging over short, modified periodograms," *IEEE Transactions on Audio and Electroacoustics*, vol. AU-15, pp. 17–20, June 1967.

[13] P. S. Moses and Randolph, *Spectral Analysis of Signals*, 1st ed. New Jersey: Prentice Hall, 2004.